Electronic Supplementary Material (ESI) for Lab on a Chip.
This journal is © The Royal Society of Chemistry 2021

Electronic Supplementary Information (ESI) for:

Exploring early time points of vimentin assembly in flow with fluorescence fluctuation spectroscopy

Eleonora Perego[a] and Sarah Köster[a,b*]

Vimentin filaments assembled at different labeling ratios

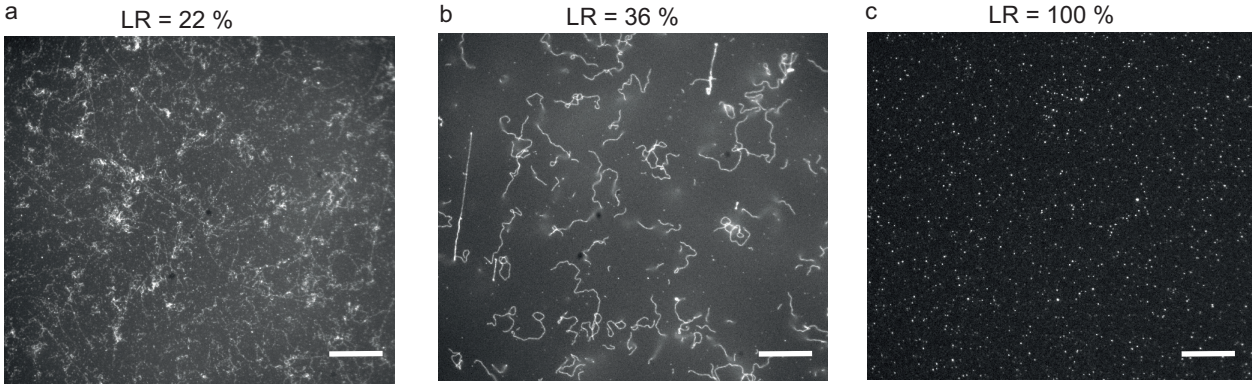

Figure S1 Vimentin filaments are assembled by mixing vimentin tetramers (c = 0.7 g/L for LR = 22%, c = 0.4 g/L for LR = 36% and c = 0.4 g/L for LR = 100%) with assembly buffer to a final concentration of 100 mM KCl in 2 mM PB, pH 7.5. The fluorescence images are taken after 9 h of *in vitro* assembly at 37 °C. a,b) When 22% or 36% of vimentin monomers are labeled, filaments are properly formed, whereas c) if only labeled monomers are assembled (LR = 100%), no vimentin filaments are visible in the microscopy images. The scale bars are 20 μm.

[a] *Institute for X-Ray Physics, University of Göttingen, 37077 Göttingen*; [b] *Cluster of Excellence "Multiscale Bioimaging: from Molecular Machines to Networks of Excitable Cells" (MBExC), University of Göttingen, Germany*
[*] *E-Mail: sarah.koester@phys.uni-goettingen.de*

Wafer production for the microfluidic step device

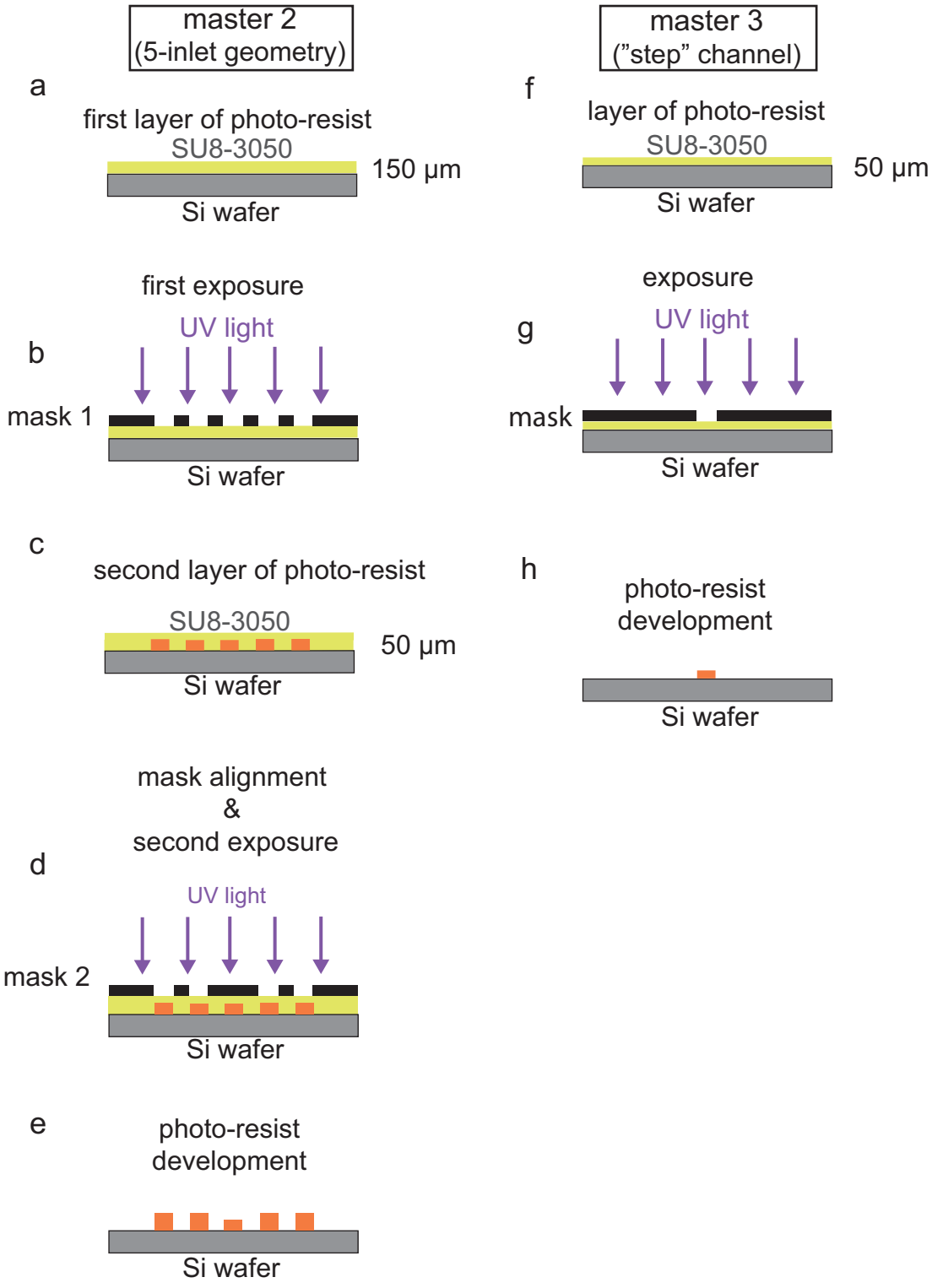

Figure S2 Step-by-step photo-lithography procedure for producing the microfluidic step device (device B) employed to study vimentin assembly. Two different wafers are produced. Master 2 is employed to create the five-inlet geometry (width = 200 μm, height = 150 μm for the central inlet and height = 200 μm for the remaining channels). Master 3 is employed to create the "step" for the protein inlet (width = 200 μm, height = 50 μm), used in the next steps of the protocol to create the channel constriction. For master 2, in order to obtain a central channel with a different height than the rest of the geometry, two layers of photo-resist are subsequently spin-coated, aligned and exposed.

Fabrication of the microfluidic step device

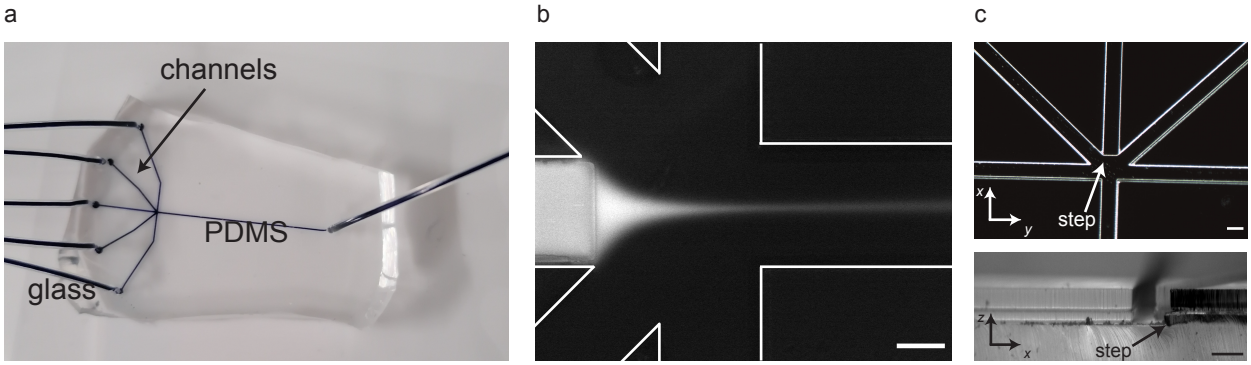

Figure S3 a) Photograph of the fully assembled microfluidic device. To better display the channel geometry, the device is filled with ink. b) Fluorescence micrograph of hydrodynamically focused, labeled vimentin tetramers with a concentration of 0.1 g/L in the microfluidic device. Note that the vimentin concentration is 300 times higher than in the flow assembly experiments to be able to visualize the stream. The scale bar is 100 μm. c) Bright field image (taken with a stereo microscope) of the PDMS part of the 5-inlet device: top view (top), side view (bottom). In both images the step is indicated by the arrows. The scale bars are 200 μm.

FEM simulation for the step device at slow flow rates

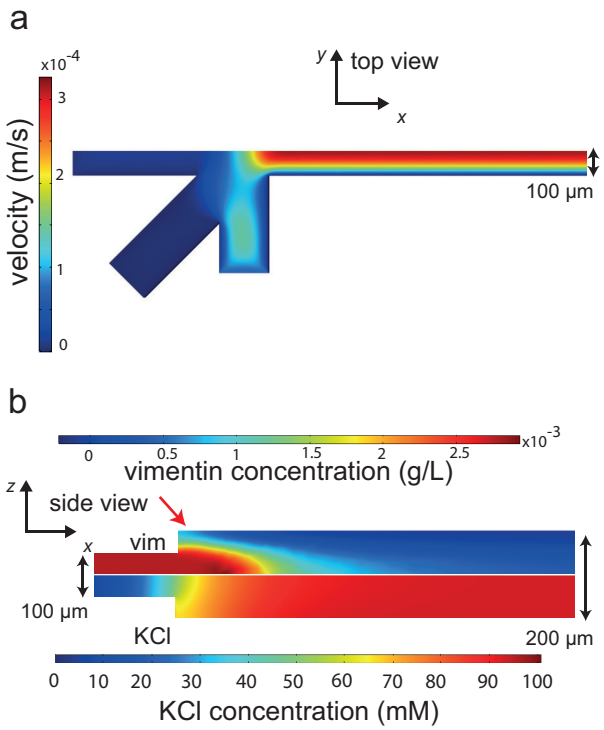

Figure S4 FEM simulation of the step device (device B) at slow flow rates (7 μm/s for the central inlet, 2 μm/s for the diagonal inlets and 65 μm for the side inlets which correspond to flow rates of 0.5 μL/h, 0.3 μL/h and 9.3 μL/h, respectively). a) Flow velocity in the central x-y plane of the device. In this case the maximum velocity in the center of the device is 0.3 mm/s. At this flow velocity, it may be possible to quantify the diffusion coefficient of vimentin tetramers with FCS in the microfluidic device. b) Central x-z plane of the device. Vimentin and KCl concentration are shown in the top and in the bottom half of the subfigure, respectively. At these flow rates, vimentin is in contact with the channel wall (red arrow) in the cross section of the device.

FFS measurements of vimentin tetramers

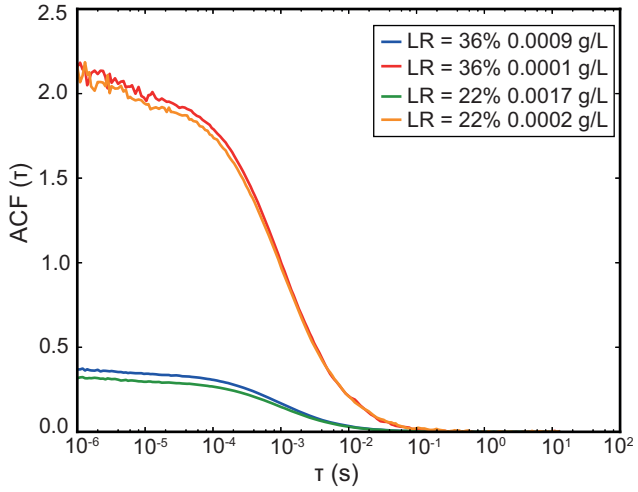

Figure S5 FCS measurements of vimentin tetramers in bulk at different concentrations and labeling ratios. The analysis is performed on the same data set as shown in Fig. 4a in the main text for the PCH analysis. The FCS curves are the average of 10 runs with 30 s of acquisition time each. The results for the number of fluorescently labeled objects in the observation volume, N_{PCH}, obtained by PCH analysis are in agreement with the results from the FCS fits N_{FCS}. An average diffusion coefficient of $\langle D \rangle$ = 27 $\pm$ 2 μm^2/s, comparable to previous measurements on vimentin tetramers[1] and with the value calculated value using the Stokes-Einstein equation[2,3] (D = 24 μm^2/s) is obtained (see Table S1).

LR (%)	c_{vim} (g/L)	N_{PCH}	N_{FCS}	D (μm^2/s)
22	0.0017	1.36 $\pm$ 0.08	1.201 $\pm$ 0.008	27 $\pm$ 2
22	0.0002	0.14 $\pm$ 0.02	0.1739 $\pm$ 0.0007	29 $\pm$ 2
36	0.0009	1.01 $\pm$ 0.04	1.04 $\pm$ 0.01	26 $\pm$ 2
36	0.0001	0.14 $\pm$ 0.04	0.1736 $\pm$ 0.0007	29 $\pm$ 1

Table S1 Summary of the fit parameters of the curves shown in Fig. S5† and in Fig. 4a in the main text.

Assembly of vimentin tetramers with a labeling ratio of 40%

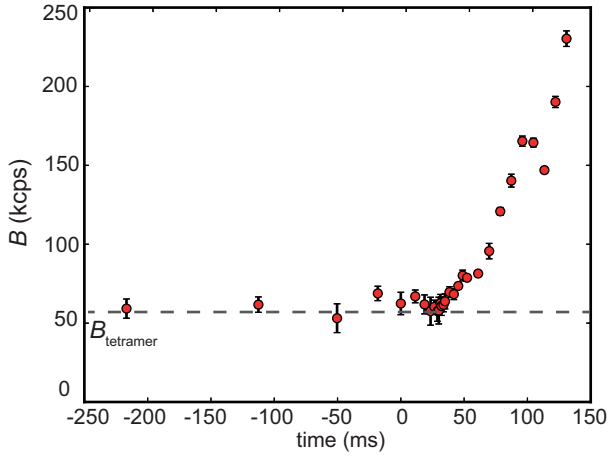

Figure S6 Assembly of vimentin tetramers with a labeling ratio of 40% in a microfluidic step device. Brightness plotted against time during assembly. The x-axis represents the reaction time calculated from the measurement positions. Note that before time 0 the brightness is constant to a value corresponding to the tetrameric stage (dotted line, $B = 55 \pm 5$ kcps, measured in bulk). The experiment is stopped at around 150 ms of assembly, thus the ULFs plateau is not present here. The error bars denote the fitting errors.

Second brightness component observed during vimentin assembly using microfluidics

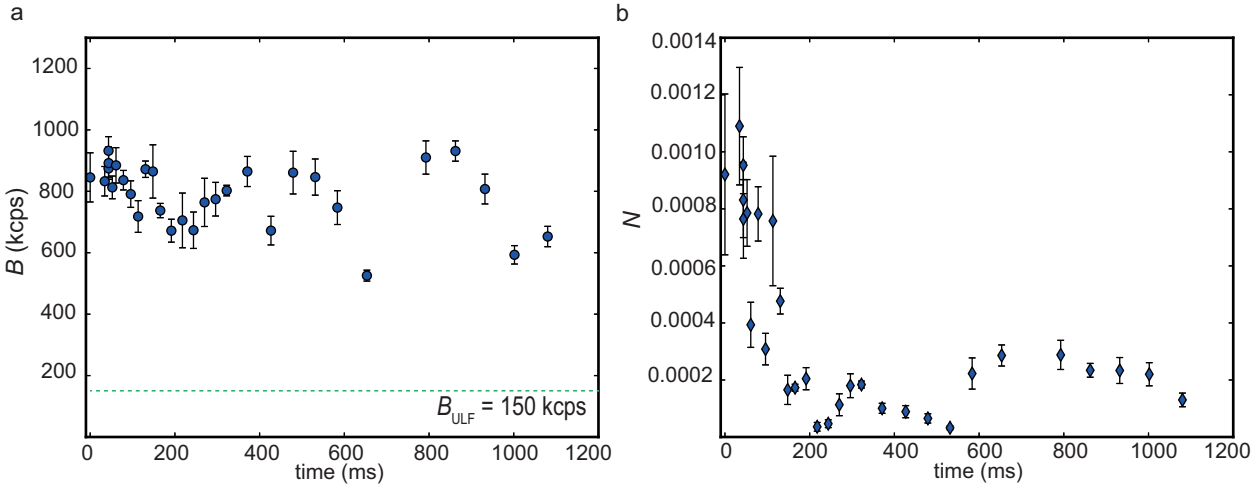

Figure S7 Second brightness component measured with PCH for vimentin assembling in device B. For the vimentin experiments performed in the step device, a two-component model is necessary to describe the PCH data. The brightness of this second component is much higher than the expected brightness for ULFs, indicating the possible presence of disordered protein aggregates in the sample. The average number of molecules in the observation volume is very low, at least 20 times lower than for the vimentin assemblies. This second component is only measured during vimentin assembling experiments, it is not present with other samples in the device, as rhodamine 6G, Alexa-532 or Atto-532 maleimide.

Fluorescence Fluctuation Spectroscopy

Fluorescence Fluctuation Spectroscopy (FFS) is a family of techniques which take advantages of temporal fluctuations in the fluorescence signal. To measure local changes in concentration of the

molecules of interest within the excited volume, which usually are the cause of the intensity fluctuations, it is important to ensure a low concentration of emitters and a small confined excitation volume. Fluorescence Correlations Spectroscopy (FCS) and Photon Counting Histogram (PCH) are two members of the FFS family and described in detail in the following.

Fluorescence Correlation Spectroscopy

Fluorescence Correlation Spectroscopy (FCS) is a versatile technique based on the analysis of fluorescence fluctuations over time within a defined excitation volume[3]. These fluctuations are the result of molecular dynamics in the excitation volume. The main cause is typically the Brownian motion of molecules moving across the observation volume, however, convective flow also affects the fluctuations.

FCS is employed to characterize the mobility of fluorescently labeled molecules. The fluorescence intensity $F(t)$ recorded from a confined volume is correlated over time to calculate the autocorrelation function ACF(τ),

$$\mathrm{ACF}(\tau) = \frac{\langle \delta F(t) \cdot \delta F(t+\tau) \rangle}{\langle F(t) \rangle^2},$$

where $\delta F(t)$ represents the fluctuations of fluorescence intensity with respect to the average value $\langle F(t) \rangle$ in a certain time t: $\delta F(t) = F(t) - \langle F(t) \rangle$, and τ is the time delay relative to an earlier time point in the measurement, or the lag-time. The resulting ACF depicts the time correlation of the fluorescence intensity as a function of the particle number N and the diffusion time $\tau_D = w_0/4D$,

$$\mathrm{ACF}(\tau) = \frac{\gamma}{N} \frac{1}{1+\frac{\tau}{\tau_D}} \frac{1}{\sqrt{1+\frac{\tau}{\tau_D}(\frac{w_0}{z_0})^2}} = \frac{\gamma}{N} G(\tau), \tag{S1}$$

where w_0 and z_0 are the beam profile parameters of the observation volume, D is the diffusion coefficient, and γ is the illumination profile factor, which in our case for confocal microscopy (one photon excitation, OPE) is 0.35. In our experiments, the width of the observation volume is typically $w_0 = (310 \pm 10)$ nm and $z_0 = 1.9$ μm, measured at 22 °C.

When two diffusing components are present in the sample, the ACF can be described as[3],

$$\mathrm{ACF}_2(\tau) = \frac{\gamma}{N^2}\big(N_1 G_1(\tau) + N_2 G_2(\tau)\big), \tag{S2}$$

where N_1 and N_2 are the average numbers of fluorescently labeled objects of each species, $N = N_1 + N_2$ is the total number of diffusing objects and $G_1(\tau)$ and $G_2(\tau)$ correspond to the single species, see eqn. (S1).

When convective flow is present, the fluorescent molecules move with a velocity v, the ACF gains an additional component,

$$\mathrm{ACF}(\tau)_{\mathrm{flow}} = G(\tau) \cdot \exp\big(-(\frac{\tau}{\tau_\mathrm{F}})^2 \cdot (1+\frac{\tau}{\tau_D})^2\big), \tag{S3}$$

where, $\tau_\mathrm{F} = \frac{w_0}{v}$ is the time decay due to the convective flow and $G(\tau)$ corresponds to the single species diffusive model, see eqn. (S1). Note that, if v is too high ($\tau_D >> \tau_\mathrm{F}$) the contribution of diffusion becomes negligible and thus FCS cannot be used to measure diffusion. For this reason, when FCS is employed on our microfluidic device, only the flow velocity and the average number of fluorescent molecules in the observation volume can be quantified.

Photon Counting Histogram

The same fluorescence fluctuation data recorded for FCS can also be used to generate a photon counting histograms (PCH). Instead of correlating the fluctuations of intensity over time, the frequencies of the intensities of the fluorescence signal are considered and a histogram of the fluctuation intensities is calculated. PCH provides quantitative information about the average number of fluorescently labeled molecules in the observation volume and about the brightness of these molecules[3]. If a sample contains two types of molecules with the same diffusion coefficient but a different number of fluorescent labels attached, it would be impossible to distinguish the two populations based on FCS only. However, the two types of molecules emit different fluorescence intensities with distinct brightness and therefore it is possible to distinguish them by PCH.

A constant light intensity source generates a photon counting histogram which follows Poissonian statistics and is described by Mandel's formula[4]:

$$p(k,t,T) = \int_0^\infty \frac{(\eta_W W(t))^k e^{-\eta_W W(t)}}{k!} p(W(t)) dW(t). \tag{S4}$$

Here, $p(k,t,T)$ is the probability of observing k photoelectrons at time t, which depends on the detection efficiency η_W, the integration time T and the energy distribution $p(W(t))$. $W(t)$ represents the light energy falling on the detector. As our typical samples are constituted by fluorescent molecules diffusing through the observation volume and not by a constant light source, the photon counting histogram calculated from the intensity fluctuations is described by a super-Poissonian distribution, with a larger variance than a Poisson distribution. The molecular brightness is defined as $b = I_0 \beta \eta T$, where I_0 is the intensity emitted by a particle located in the center of the observation volume, β represents factors related to the optical setup, η is the detection efficiency and T is the binning time. Thus, it represents the intensity measured on the detector which is emitted from a particle in the center of the PSF during one integration time T. It depends on the detection optics and the integration time. PCH can also be applied in combination with microfluidics. As long as undersampling is avoided, flow does not affect the photon distribution[5]. Therefore, as long as the integration time T is shorter than the time scale of the considered fluorescence fluctuations, the shape of PCH is independent of the flow.

References

[1] A. Robert, M. J. Rossow, C. Hookway, S. A. Adam and V. I. Gelfand, *Proc. Natl. Acad. Sci. U. S. A.*, 2015, **112**, E3505–E3514.

[2] M. E. Young, P. A. Carroad and R. L. Bell, *Biotechnol. Bioeng.*, 1980, **22**, 947–955.

[3] J. R. Lakowicz, *Principles of Fluorescence Spectroscopy*, Springer,, New York, 3rd edn, 2006.

[4] Y. Chen, J. D. Müller, P. T. C. So and E. Gratton, *Biophys. J.*, 1999, **77**, 553–567.

[5] J. Johnson, Y. Chen and J. D. Müller, *Biophys. J.*, 2010, **99**, 3084–3092.